IEEE Access
Multidisciplinary | Rapid Review | Open Access Journal

Received October 11, 2018, accepted October 25, 2018, date of publication October 31, 2018, date of current version November 30, 2018.

Digital Object Identifier 10.1109/ACCESS.2018.2878811

Optimal Sculling Velocity Algorithms for the Gyros With Angular Rate Output

LEI HUANG[1,2,3], FEI XIE[3,4], AND KAI FENG[1]

[1]School of Mechanical and Electrical Engineering, Nanjing Forestry University, Nanjing 210037, China
[2]School of Instrument Science and Engineering, Southeast University, Nanjing 210096, China
[3]Jiangsu Key Laboratory of 3D Printing Equipment and Manufacturing, Nanjing Normal University, Nanjing 210037, China
[4]School of Electrical and Automation Engineering, Nanjing Normal University, Nanjing 210042, China

Corresponding author: Fei Xie (xiefei@njnu.edu.cn)

This work was supported in part by the National Natural Science Foundation of China under Grant 51305207 and Grant 61601228, in part by the Natural Science Foundation of Jiangsu Provincial College under Grant 13KJB460010, in part by the Natural Science Foundation of Jiangsu under Grant BK20161021, and in part by the Top-notch Academic Programs Project of Jiangsu Higher Education Institutions under Grant PPZY2015A062.

ABSTRACT With the advance of gyro technology, modern gyros have two output types: angular rate or integrated angular rate. However, the conventional sculling velocity algorithms usually still adopt integrated angular rate/specific-force increments as algorithm inputs. So the engineer must convert the angular rate into integrated angular rate by digital integration to use them. This step will produce non-negligible computational error. To solve this issue, we proposed two types of novel optimal sculling algorithms using angular rate input. The advantage of the novel algorithms is that they can directly calculate out the carrier velocity without converting the angular rate of gyro output into integrated angular rate. Hence, they have a higher accuracy than the conventional sculling algorithms. The results of digital simulations also demonstrate this conclusion.

INDEX TERMS Strapdown inertial navigation algorithm, velocity algorithm, sculling algorithm, coning algorithm, specific-force transformation.

NOMENCLATURE

f	= specific-force measured by accelerometers
C_b^n	= direction cosine matrix
H	= update period
h	= subminor interval in one update period
$\Delta\theta_i$	= incremental angle vector over the ith subminor interval
ω_{A1A2}^{A3}	= angular rate of coordinate frame $A2$ relative to coordinate frame $A1$ projected on $A3$ frame axe; when $A1$ is the inertial I frame, ω_{A1A2} is the angular rate measured by angular rate sensors mounted on frame $A2$

I. INTRODUCTION

A. RELATED RESEARCH WORK

Nowadays, strapdown inertial navigation systems (SINS) such as being installed on a high-speed unmanned surface vehicle (USV), often work in a high dynamic environment. To assess the performance of the navigation algorithms used in SINS, some standard carrier motions are employed. For example, coning motion is the standard input to assess the performance of the strapdown attitude algorithm, sculling motion is the standard input to assess the performance of the strapdown velocity algorithm under highly dynamic environments. To improve the navigation accuracy of SINS in the high dynamic environment, many scholars conducted numerous researches. Among them Savage is the most outstanding scholar. He provided an analytical description of sculling motion and proposed a collection of algorithms which can preciously calculate the coning correction and the sculling correction [1], [2]. He also give an analytical model for the evaluation of error build-up under band-limited random process input for the digital integration coning and sculling algorithm [3], [4]. It was demonstrated that the digital integration process introduced a random walk type error in the output that was directly proportional to the rootmean-square input amplitude, directly proportional to the square-root of the input bandwidth, and inversely proportional to the digital integration update frequency. Ignagni is another famous scholar. He derived a class of optimized sculling algorithms and demonstrated a duality between the derived class of sculling algorithms and the class of coning algorithms [4]–[6]. Roscoe proposed a generic equivalency between coning and

sculling integrals and algorithms. Following his method, it is easy to obtain a sculling algorithm from the corresponding coning algorithm based on incremental angle input by adopting a simple mathematical formula [7]. In [8] two alternative approaches were developed for deriving strapdown navigation sculling algorithms. A key point of the two approaches is the uses of additional gyro/accelerometer output signals which are the increments of the angular-rate/specific-force multiple integrals over the iteration interval to improve the algorithm accuracy. Song employed Taylor series expansion to analyze the error of the conventional sculling correction algorithm under maneuvers, he proposed some new sculling algorithms which are constructed with the presented sculling algorithms for the velocity translation vector, and avoid the loss in accuracy of velocity translation vector under maneuvers [9], [10].

B. KEY WORK OF THIS PAPER

These conventional sculling velocity algorithms are all based on the assumption that the output of gyro is integrated angular rate. However, modern inertial sensors produce different types of output now. For example, the micro-electromechanical systems (MEMS) gyro and some kinds of fiber optical gyro (FOG) have angular rate sampled output, not integrated angular rate. So, the conventional sculling velocity algorithms are not well-suited for the SINS which are equipped with a FOG or a MEMS gyro. In addition, at the present the accelerators also have different output types, for example, the quartz accelerometer output is usually specific-force, but some other types of accelerometer output specific-force increments.

In order to adapt to this tendency, we designed two types of optimal sculling velocity algorithms based on angular rate input. The first type of algorithms uses the angular rate/specific-force as the algorithm inputs. The second uses the angular rate/specific-force increments as algorithm inputs. These novel algorithms can directly calculate out the carrier velocity without converting the dimension of gyro's output. Therefore, for the SINS equipped with a gyro with the output of angular rate, the precision of the algorithm can be improved considerably.

II. ALGORITHM EXAMPLES FOR CONVENTIONAL SCULLING ALGORITHMS

Velocity rate equation is [1]:

$$\dot{V} = C_b^n f - (2\omega_{ie}^n + \omega_{en}^n) \times V^n + g^n \tag{1}$$

where g^n is the gravitational acceleration projected on "n" frame axe (navigation coordinate). The subscripts "i, e, n" in ω represent the inertial coordinate, geographic coordinate, and navigation coordinate respectively. "V" is the carrier velocity. The body's velocity in navigation coordinates at time t_m is then obtained as the integral of Eq.(1) from time t_{m-1}, evaluated at time t_m:

$$\begin{aligned} V_m^n &= V_{m-1}^n + C_{b(m-1)}^{n(m-1)} \int_{t_{m-1}}^{t_m} C_{b(t)}^{b(m-1)} f dt \\ &\quad + \int_{t_{m-1}}^{t_m} [g^n - (2\omega_{ie}^n + \omega_{en}^n) \times V_{m-1}^n] dt \\ &= V_{m-1}^n + C_{m-1} \Delta V_{sfm} + \Delta V_{g/corn} \end{aligned} \tag{2}$$

where m is the digital velocity integration algorithm update rate computer cycle index, ΔV_{sfm} is the integrated transformed specific-force increment, $\Delta V_{g/corn}$ is the gravity/Coriolis velocity increment. g^n, ω_{ie}^n in $\Delta V_{g/corn}$ can be assumed as constants. Hence $\Delta V_{g/corn}$ in Eq. (2) can be calculated approximately as a constant during one update period. ω_{en}^n is almost no variation during (t_{m-1}, t_m) so it can be derived from the V_{m-1}^n, which is the carrier velocity at t_{m-1} and has been calculated out during the last velocity determination iteration. The ΔV_{sfm} calculation includes solving for an integral that represents the change in velocity caused by specific-force acceleration ([1], Eq.(26)):

$$\Delta V_{sfm} = \Delta V_m + \int_{t_{m-1}}^{t_m} (\Delta\theta(t) \times f(t)) dt \tag{3}$$

where:

$$\Delta\theta(t) = \int \omega(t) dt, \; \Delta V_m = \int_{t_{m-1}}^{t_m} f(t) dt \tag{4}$$

Then, Eq. (3) can be written as [see [1], Eqs. (27–36) for development]:

$$\begin{aligned} \Delta V_{sfm} &= \Delta V_m + \frac{1}{2} \Delta\theta_m \times \Delta V_m \\ &\quad + \frac{1}{2} \int_{t_{m-1}}^{t_m} [\Delta\theta(t) \times f(t) + \Delta V(t) \times \omega(t)] dt \\ &= \Delta V_m + \Delta V_{rotm} + \Delta V_{sculm} \end{aligned} \tag{5}$$

where ΔV_{rotm} is the velocity rotation correction and ΔV_{sculm} is the sculling correction. Obviously, there is:

$$\Delta v_{sculm} = \frac{1}{2} \int_{t_{m-1}}^{t_m} [\Delta\theta(t) \times f + \Delta V(t) \times \omega] dt \tag{6}$$

The discrete algorithm of ΔV_{sculm} can be converted from coning algorithm using a simple duality formula [5], [7]. For example, the 2-interval optimal sculling algorithm using incremental angle/specific-force increments inputs is [5], [7]:

$$\Delta \hat{V}_{sculm} = \frac{2}{3} (\Delta\theta_1 \times \Delta V_2 + \Delta V_1 \times \Delta\theta_2) \tag{7}$$

Its coning algorithm counterpart, namely the 2-interval optimal coning algorithm using incremental angle input is [1], [5]:

$$\Delta\Phi = \frac{2}{3} (\Delta\theta_1 \times \Delta\theta_2) \tag{8}$$

The 3-interval optimal sculling algorithm is [5], [7]:

$$\begin{aligned} \Delta \hat{V}_{sculm} &= (\frac{9}{20} \Delta\theta_1 + \frac{27}{20} \Delta\theta_2) \times \Delta V_3 \\ &\quad + (\frac{9}{20} \Delta V_1 + \frac{27}{20} \Delta V_2) \times \Delta\theta_3 \end{aligned} \tag{9}$$

Its coning algorithm counterpart, namely the 3-interval optimal coning algorithm [5], [7]:

$$\Delta\Phi = (\frac{9}{20}\Delta\theta_1 + \frac{27}{20}\Delta\theta_2) \times \Delta\theta_3 \tag{10}$$

III. SCULLING ALGORITHM USING ANGULAR RATE/SPECIFIC-FORCE INPUT

There are two imperfections in the conventional sculling velocity algorithms such as [5] and [7]. Firstly, strictly speaking, only with the duality between coning integral and sculling integral we can't obtain the optimal coefficients for the sculling integration algorithm. To obtain the optimal coefficients, the duality between true coning correction and true sculling correction also needs to be demonstrated. Secondly, as is seen in Eqs.(7) and (10), the conventional sculling algorithm adopts the integrated angular-rate/specific-force increments as input. But with the development of inertial sensors, many inertial measurement units (IMU) have the output of angular rate now. In such cases the conventional sculling algorithms can't calculate the body's velocity accurately. To use the conventional velocity algorithms, we must convert the angular rate into incremental angle by digital integration in order to use Eq.(7) or Eq.(9). Obviously, this step will cause the non-negligible computational error. To solve this problem, we proposed two types of formalized optimal sculling algorithm based on angular rate input in this paper. The first type is the optimal sculling algorithm based on angular rate/specific-force inputs. The derivation process is based on the duality between the coning integral and the sculling integral as well as the duality between true coning correction and true sculling correction.

A. THE DUALITY BETWEEN THE GENERIC CONING INTEGRAL AND SCULLING INTEGRAL

Let us define $\Delta\hat{V}_{sculm}$ to be a digital integration algorithm for sculling correction, $\hat{\beta}$ be a digital integration algorithm for coning correction. Reference [5] has demonstrated the duality equivalency between the generic coning integral and sculling integral. The demonstration details in [5] can be seen in Appendix. From [6] (Eq.(25)) we can obtain the generic coning integral term using angular rate input:

$$\hat{\beta} = \sum_{j=i+1}^{N}\sum_{i=0}^{N-1} K_{ij}(\omega_i \times \omega_j)H^2 \tag{11}$$

where K_{ij} is the constant coefficients which will be optimized under coning motion, ω_i is the angular rate sample of ith moment in one iteration interval. Based on duality principle, from Eq.(A12) in Appendix we can obtain:

$$\begin{aligned}\Delta\hat{V}_{sculm} &= \sum_{j=i+1}^{N}\sum_{i=0}^{N-1} K_{ij}([\omega_i(t)+f_i(t)]\times[\omega_j(t)+f_j(t)])H^2 \\ &\quad - \sum_{j=i+1}^{N}\sum_{i=0}^{N-1} K_{ij}(\omega_i\times\omega_j)H^2 - \sum_{i=0}^{N-1}\sum_{j=i+1}^{N} K_{ij}(f_i\times f_j)H^2 \\ &= \sum_{j=i+1}^{N}\sum_{i=0}^{N-1} L_{ij}[\omega_i(t)\times f_j(t)]H^2\end{aligned} \tag{12}$$

where L_{ij} is the unknown coefficient which should be optimized under sculling motion.

B. THE DUALITY BETWEEN TRUE CONING CORRECTION AND TRUE SCULLING CORRECTION

However, only from the duality between the generic coning integral and the generic sculling integral in [5] we can't obtain the optimal coefficients for the sculling integration algorithm. To obtain the optimal coefficients, the duality between true coning correction and true sculling correction also needs to be demonstrated.

A typical sculling motion is defined as:

$$\omega = \mathbf{b}\Omega\cos(\Omega t)J, \quad f = \mathbf{c}\sin(\Omega t)K \tag{13}$$

where $\mathbf{b}$ is the amplitude of the angular vibration,$\mathbf{c}$ is the amplitude of the specific-force vibration, J, K are the unit vectors along the two body axes (y, z) about which the oscillations are occurring, and Ω is the frequency associated with the angular and specific-force oscillations. Substituting Eq.(13) into Eq.(6) gives the true sculling correction:

$$\begin{aligned}\Delta V_{sculm} &= \frac{1}{2}\int_{t_{m-1}}^{t_m}[\Delta\theta(t)\times f + \Delta V(t)\times\omega]dt \\ &= \frac{\mathbf{bc}}{2}(H - \frac{1}{\Omega}\sin\Omega H)I\end{aligned} \tag{14}$$

where H is the algorithm update period $H = t_m$-t_{m-1}.

A typical coning motion is defined as [11]:

$$\omega = [0, \mathbf{a}\Omega\cos(\Omega t)J, \mathbf{d}\Omega\sin(\Omega t)K] \tag{15}$$

where $\mathbf{a}$, $\mathbf{d}$ are the amplitudes of the angular oscillations in two orthogonal axes of the body. Ω is the frequency associated with the angular oscillations. The corresponding true coning correction is [5], [7]:

$$\beta = \frac{\mathbf{ad}}{2}(\Omega H - \sin\Omega H)I \tag{16}$$

Compared Eq. (14) with Eq. (16), we can find that Eq. (14) equals Eq. (16) when $\mathbf{b}$ in Eq. (14) are replaced by $\mathbf{a}$, and $\mathbf{c}$ in Eq. (14) are replaced by $\mathbf{d}\Omega$. This is because the coning motion equation Eq. (13) equals the sculling equation Eq. (15) when $\mathbf{b}$ in Eq. (13) is replaced by $\mathbf{a}$, and $\mathbf{c}$ in Eq. (13) is replaced by $\mathbf{d}\Omega$. Hence there is a duality between true coning correction and true sculling correction.

C. THE EQUIVALENCE BETWEEN THE OPTIMAL COEFFICIENTS OF CONING AND OF SCULLING ALGORITHMS

The sculling integral should equal the true sculling correction in a sculling environment.

$$\Delta\hat{V}_{sculm} = \Delta V_{sculm} \tag{17}$$

Also, the coning integral term given in Eq. (11) should equal the true coning correction in a coning environment. There is:

$$\hat{\beta} = \beta \tag{18}$$

As is stated, there are dualities between $\Delta\hat{V}_{sculm}$ and $\hat{\beta}$, ΔV_{sculm} and β. Hence the optimal coefficients of sculling algorithm using angular rate/specific-force input are equivalent to those of coning algorithm using angular rate input. The optimal coefficients of coning algorithms using angular rate input have been derived in [4] [Eqs.(33), (36), and (42)]. So it is easy to obtain the corresponding sculling algorithm.

D. ALGORITHM EXAMPLES

This section converts two existing derived coning algorithms into their sculling algorithm counterparts.

1) EXAMPLE 1 2-INTERVAL OPTIMAL SCULLING ALGORITHM

In [4, eq. (47)], the 2-interval optimal coning algorithm using angular rate input is:

$$\hat{\beta} = \frac{h^2}{45}(\omega_0 \times \omega_2) + \frac{28h^2}{45}(\omega_1 \times \omega_2) \tag{19}$$

where h is the sub-minor interval of the algorithm. For a 2-interval algorithm there is $H{=}2h$. According to Eq.(19) and Eq.(A12) the 2-interval optimal sculling algorithm using angular rate/specific-force input can be obtained:

$$\begin{aligned}\Delta\hat{V}_{sculm} = {} & \frac{H^2}{180}(\omega_0 \times f_2 + f_0 \times \omega_2) \\ & + \frac{7H^2}{45}(\omega_0 \times f_1 + f_0 \times \omega_1)\end{aligned} \tag{20}$$

2) EXAMPLE 2 3-INTERVAL OPTIMAL SCULLING ALGORITHM

In [4, eq. (45)], the 3-interval optimal coning algorithm using angular rate input is given as:

$$\hat{\beta} = \frac{87h^2}{2240}(\omega_0 \times \omega_3) + \frac{27h^2}{56}(\omega_1 \times \omega_3) + \frac{2619h^2}{2240}(\omega_2 \times \omega_3) \tag{21}$$

where h is the subminor interval of the algorithm. For a 3-interval algorithm there is $H{=}3h$. According to Eq.(21) and Eq.(A12) the 3-interval optimal sculling algorithm using angular rate/specific-force input can be obtained:

$$\begin{aligned}\Delta\hat{V}_{sculm} = {} & \frac{29H^2}{6720}(\omega_0 \times f_3 + f_0 \times \omega_3) \\ & + \frac{3H^2}{56}(\omega_1 \times f_3 + f_1 \times \omega_3) \\ & + \frac{291H^2}{2240}(\omega_2 \times f_3 + f_2 \times \omega_3)\end{aligned} \tag{22}$$

E. DIGITAL INTEGRATION ALGORITHM FOR VELOCITY ROTATION

$\Delta\theta_m$, ΔV_m in Eq.(5) can be calculated by digital integration. For example for a 2-interval system there is:

$$\Delta\theta_m = (\frac{\omega_0}{6} + \frac{4\omega_1}{6} + \frac{\omega_2}{6})H,\ \Delta V_m = (\frac{f_0}{6} + \frac{4f_1}{6} + \frac{f_2}{6})H \tag{23}$$

Substituting Eq.(23) into Eq.(5) gives the velocity rotation correction ΔV_{rotm} of 2-interval velocity rotation digital integration algorithm:

$$\hat{V}_{rotm} = \frac{1}{2}(\frac{\omega_0}{6} + \frac{4\omega_1}{6} + \frac{\omega_2}{6}) \times (\frac{f_0}{6} + \frac{4f_1}{6} + \frac{f_2}{6})H^2 \tag{24}$$

Then substituting Eqs.(23), (24) and (20) into Eq.(5), we obtain the integrated transformed specific-force increment ΔV_{sfm} of a 2-interval system there:

$$\begin{aligned}\Delta v_{sfm} = {} & \upsilon_m + \Delta v_{rotm} + \Delta v_{sculm} \\ = {} & (\frac{f_0}{6} + \frac{4f_1}{6} + \frac{f_2}{6})H + \frac{1}{2}(\frac{\omega_0}{6} + \frac{4\omega_1}{6} + \frac{\omega_2}{6}) \\ & \times (\frac{f_0}{6} + \frac{4f_1}{6} + \frac{f_2}{6})H^2 \\ & + \frac{H^2}{180}(\omega_0 \times f_2 + f_0 \times \omega_2) + \frac{7H^2}{45}(\omega_0 \\ & \times f_1 + f_0 \times \omega_1)\end{aligned} \tag{25}$$

Described previously, $\Delta V_{g/corn}$ in Eq. (2) can be calculated approximately as a constant. Considering V^n_{m-1} in Eq. (2), *i.e.*, the carrier velocity at t_{m-1} has been calculated out during the last velocity determination iteration. By substituting Eq.(25) into Eq.(2) the carrier velocity at t_m, *i.e.*, V^n_m will be achieved.

IV. SCULLING ALGORITHM USING ANGULAR RATE/SPECIFIC-FORCE INCREMENTS INPUT

As is stated, some types of accelerometer have the output of specific-force increments now. If the IMU produce angular rate/specific-force increments outputs, the conventional sculling algorithms such as Eqs.(7) and (9) cannot calculate out the carrier's velocity directly. The sculling velocity algorithm must include a step for converting angular rate into integrated angular rate by digital integration. This step will produce non-negligible computational error. To solve this problem, we have developed a novel sculling algorithm using angular rate/specific-force increments input directly.

A. FORMALIZED OPTIMAL SCULLING ALGORITHM

For an N-interval sculling velocity algorithm using angular rate/specific-force increment inputs, the sample number of the accelerometer outputs (specific force) is $N+1$, and the number of the gyro outputs (integrated angular rate) is N. The theoretical gyro/accelerometer outputs in a sculling environment defined by Eq.(15) are:

$$\begin{cases}\omega_i = \mathbf{b}\Omega \\ \quad \times \cos[\Omega(t_m + \dfrac{i-1}{N}H)]J, & i = 1, 2, \ldots, N+1 \\ \Delta V_j = \dfrac{2\mathbf{c}}{\Omega}\sin\dfrac{\Omega H}{2N} \\ \quad \times \sin\Omega[t_{m-1} + \dfrac{(2j-1)H}{2N}]K, & j = 1, 2, \ldots, N\end{cases} \tag{26}$$

Based on the duality between coning correction and sculling correction, following the derivation of

Eqs.(A8)-(A12) in Appendix, we can obtain:

$$\Delta\hat{V}_{sculm} = \Delta\hat{\Phi}([\omega + \Delta V] \to \omega) - \Delta\hat{\Phi} - \Delta\hat{\Phi}(\Delta V \to \omega) \tag{27}$$

where "A→B" represents the "B replaced by A". For example, "$\omega + \Delta V \to \omega$" means that ω is replaced by $\omega + \Delta V$. Then substituting Eq.(27) into Eq.(11) gives the generalized form of the sculling correction using angular rate/specific-force increment input:

$$\begin{aligned}
&\Delta\hat{V}_{sculm} \\
&= \sum_{j=i+1}^{N}\sum_{i=1}^{N-1} K_{ij}(\omega_i H + \Delta V_i) \times (\omega_j H + \Delta V_j) \\
&\quad - \sum_{j=i+1}^{N}\sum_{i=1}^{N-1} K_{ij}(\omega_i \times \omega_j)H^2 - \sum_{j=i+1}^{N}\sum_{i=0}^{N-1} K_{ij}(\Delta V_i \times \Delta V_j) \\
&= \sum_{j=i+1}^{N}\sum_{i=1}^{N-1} k_{ij}(\omega_i \times \Delta V_j - \omega_j \times \Delta V_i)H
\end{aligned} \tag{28}$$

where N is the number of iteration intervals over the velocity update period. It follows from Eq.(26) that:

$$\begin{aligned}
&(\omega_i \times \Delta V_j - \omega_j \times \Delta V_i)H \\
&= bcH \sin\frac{\Omega H}{2N}[\sin(\frac{2j-2i+1}{2N}\Omega H) - \sin(\frac{2i-2j+1}{2N}\Omega H)] \\
&= bcH \sin\frac{\Omega H}{N}\sin(\frac{j-i}{N}\Omega H)
\end{aligned} \tag{29}$$

Obviously, the sculling correction ΔV_{sculm} is only determined by $|j\text{-}i|$. Therefore Eq.(28) can be simplified as:

$$\Delta\hat{V}_{sculm} = \sum_{j=2}^{N} k_{j-1}(\omega_1 \times \Delta V_j - \omega_j \times \Delta V_1)H \tag{30}$$

Substituting Eq.(26) into Eq.(30) gives:

$$\Delta\hat{V}_{sculm} = \mathbf{bc}H\sum_{l=1}^{N-1} k_i \sin\frac{\Omega H}{N}\sin\frac{l\Omega H}{N} \tag{31}$$

Applying Eq.(31) with Taylor series expansion for the coefficient terms "ΩH", we obtain:

$$\begin{aligned}
\Delta\hat{V}_{sculm} = \mathbf{bc}H\{&[k_1 + 2k_2 + \cdots (N-1)k_{N-1}](\frac{\Omega H}{N})^2 \\
&+ (-\frac{k_1}{3!} - \frac{k_1}{3!} - \frac{2k_2}{3!} - \frac{2^3k_2}{3!} - \frac{3^3k_3}{3!} \\
&- \frac{3k_3}{3!}\cdots)(\frac{\Omega H}{N})^4 + \ldots\}
\end{aligned} \tag{32}$$

Applying Eq.(14) with Taylor series expansion for the coefficient terms "ΩH" gives:

$$\Delta V_{sculm} = \frac{bc}{2}[\frac{(\Omega H)^3}{3!\Omega} - \frac{(\Omega H)^5}{5!\Omega} + \cdots] \tag{33}$$

From $\Delta\hat{V}_{sculm} = \Delta V_{sculm}$ we can obtain:

$$A_{(N-1)\times(N-1)} \cdot G_{(N-1)\times 1} = D_{(N-1)\times 1} \tag{34}$$

where A and G are shown at the bottom of this page.

The solution to Eq.(34) is $G = A^{-1}D$. Details regarding the optimal coefficients are shown in Table 1.

TABLE 1. Sculling algorithm optimal coefficients.

N	$G = A^{-1}D$	$\delta\hat{V}_{sculm}$ (algorithm error in unit time)
2	$k_1 = \frac{1}{3}$	$\frac{bc}{360}(\Omega H)^4$
3	$\begin{bmatrix} k_1 \\ k_2 \end{bmatrix} = \begin{bmatrix} \frac{23}{40} & \frac{7}{80} \end{bmatrix}^T$	$\frac{17bc}{4898880}(\Omega H)^6$
…	…	…

B. ALGORITHM EXAMPLES

1) EXAMPLE 1 2-INTERVAL OPTIMAL SCULLING ALGORITHM

When N=2, substituting k_1=1/3 into Eq.(43) gives:

$$\Delta\hat{V}_{sculm} = \frac{1}{3}(\omega_1 \times \Delta V_2 - \omega_2 \times \Delta V_1)H \tag{35}$$

$$A = \underbrace{\begin{bmatrix} \frac{1}{N^2} & \frac{2}{N^2} & \cdots & \frac{N-1}{N^2} \\ \frac{1+1^3}{N^4 3!} & \frac{2+2^3}{N^4 3!} & \cdots & \frac{(N-1)+(N-1)^3}{N^4 3!} \\ \cdots & \cdots & \cdots & \cdots \\ \frac{1+1^{(2N-3)}}{N^{2(N-1)}(2N-3)!} & \frac{2+2^{(2N-3)}}{N^{2(N-1)}(2N-3)!} & \cdots & \frac{(N-1)+(N-1)^{(2N-3)}}{N^{2(N-1)}(2N-3)!} \end{bmatrix}}_{(N-1)\times(N-1)},$$

$$G = \underbrace{[k_1 k_2 \cdots k_{N-1}]^T}_{(N-1)\times 1}, D = \underbrace{\begin{bmatrix} \frac{1}{2\cdot 3!} & \frac{1}{2\cdot 5!} & \cdots & \frac{1}{2\cdot(2N-1)!} \end{bmatrix}^T}_{(N-1)\times 1}$$

The per unit time algorithm error is:

$$\delta\hat{V}_{sculm} = |\hat{V}_{sculm} - V_{sculm}| = \frac{\mathbf{bc}}{360}(\Omega H)^4 \quad (36)$$

In Eqs.(2) and (5), the integrated transformed specific-force increment ΔV_{sfm} is composed of ΔV_{sculm}, ΔV_{rotm}, and $\Delta V_{m.}\Delta V_m$ and $\Delta\theta_m$ in Eq.(5) can be calculated by digital integration:

$$\Delta\hat{\theta}_m = (\frac{\omega_1}{6} + \frac{4\omega_2}{6} + \frac{\omega_3}{6})H, \Delta\hat{V}_m = \Delta V_1 + \Delta V_2 \quad (37)$$

Substituting Eq.(37) into Eq.(5) gives:

$$\Delta\hat{V}_{rotm} = \frac{1}{2}(\frac{\omega_1}{6} + \frac{4\omega_2}{6} + \frac{\omega_3}{6}) \times (\Delta V_1 + \Delta V_2)H \quad (38)$$

Substituting Eqs. (35), (37), and (38) into Eq.(5) gives the 2-interval integrated transformed specific-force increment:

$$\Delta\hat{V}_{sfm} = \Delta V_1 + \Delta V_2 + \frac{1}{2}(\frac{\omega_1}{6} + \frac{4\omega_2}{6} + \frac{\omega_3}{6}) \times (\Delta V_1 + \Delta V_2)H + \frac{1}{3}(\omega_1 \times \Delta V_2 - \omega_2 \times \Delta V_1)H \quad (39)$$

2) EXAMPLE 2 3-INTERVAL OPTIMAL SCULLING ALGORITHM

When N=3, substituting k_1=23/40, k_2=7/80 of table 1 into Eq.(30) gives:

$$\Delta\hat{V}_{sculm} = \frac{23}{40}(\omega_1 \times \Delta V_2 - \omega_2 \times \Delta V_1)H + \frac{7}{80}(\omega_1 \times \Delta V_3 - \omega_3 \times \Delta V_1)H \quad (40)$$

For a 3-interval system there are:

$$\Delta\theta_m = (\frac{\omega_0}{8} + \frac{3\omega_1}{8} + \frac{3\omega_2}{8} + \frac{\omega_3}{8})H, \quad \Delta V_m = \Delta V_1 + \Delta V_2 + \Delta V_3 \quad (41)$$

Substituting Eq.(41) into Eq.(5) gives the velocity rotation correction ΔV_{rotm}:

$$\hat{V}_{rotm} = \frac{1}{2}(\frac{\omega_0}{8} + \frac{3\omega_1}{8} + \frac{3\omega_2}{8} + \frac{\omega_3}{8}) \times (\Delta V_1 + \Delta V_2 + \Delta V_3)H \quad (42)$$

Then substituting Eqs.(40)-(42) into Eq.(5) gives the integrated transformed specific-force increment ΔV_{sfm}:

$$\begin{aligned}\Delta v_{sfm} &= \upsilon_m + \Delta v_{rotm} + \Delta v_{sculm} \\ &= \Delta V_1 + \Delta V_2 + \Delta V_3 + \frac{1}{2}(\frac{\omega_0}{8} + \frac{3\omega_1}{8} + \frac{3\omega_2}{8} + \frac{\omega_3}{8}) \\ &\quad \times (\Delta V_1 + \Delta V_2 + \Delta V_3)H \\ &\quad + \frac{23}{40}(\omega_1 \times \Delta V_2 - \omega_2 \times \Delta V_1)H \\ &\quad + \frac{7}{80}(\omega_1 \times \Delta V_3 - \omega_3 \times \Delta V_1)H \end{aligned} \quad (43)$$

Described previously $\Delta V_{g/corn}$ in Eq. (2) can be calculated out easily, indeed it can be calculated approximatively as a constant during one update period and omitted here. V^n_{m-1} in Eq.(2), *i.e.*, the carrier velocity at t_{m-1} has been calculated out during the last algorithm update period. Thus the carrier velocity at time t_m can be calculated out by substituting Eq.(43) into Eq.(2). Comparing the proposed sculling algorithm given by Eq.(35) and (40) with the conventional sculling algorithms represented in Eqs.(**7**) and (9), we can see the advantages of the proposed algorithm are that it is able to calculate out the sculling correction, then the velocity at t_m directly without any demands for the dimension conversion of inertial sensor outputs.

V. SIMULATIONS

According to the sculling motion given by Eq.(13), we employ a 600-second digital simulation to verify the performance of the proposed sculling algorithm using angular rate/specific-force increments input. The parameters are set as: the amplitude of the angular vibration b=1°, the amplitude of the specific-force vibration c=10g, the frequency associated with the angular and specific-force oscillations Ω=2π *rad/s* (oscillation frequency is 1 *Hz*). The inertial sensors outputs are given by Eq.(26) with N=3. The velocity update period H=0.01s. The initial attitude is (0, 0, 0)°. The initial velocity is (0, 0, 0) *m/s*. The initial position is (118.78333°, 32.05000°, 10*m*). The navigation coordinate frame is set to east-north-up. The error comparisons between the proposed 3-interval sculling algorithm given by Eq.(40) and the conventional 3-interval sculling algorithm given by Eq.(**7**) are shown in Figs. 1–2. The blue and solid curve is the curve of proposed sculling algorithm errors, the red and dotted curve is the curve of conventional sculling algorithm errors.

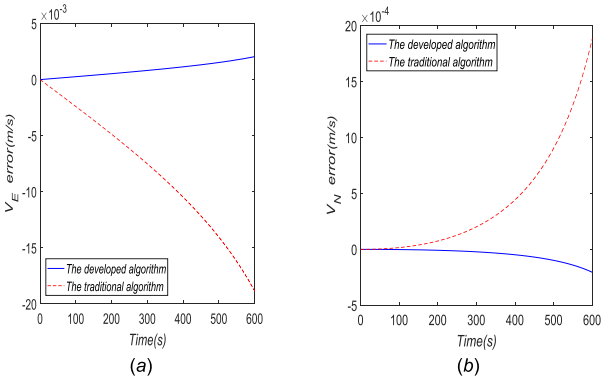

FIGURE 1. Comparison of the horizontal velocity determination results between two algorithms under sculling environment. (a) Eastward velocity error. (b) Northward velocity error.

From Fig. 1 we can see that the eastward velocity errors of both algorithms are larger about one order than northern velocity errors. This is because in a sculling environment defined by Eq.(13), the sculling error mainly exists in the x-axis of the carrier. The corresponding velocity component is V_E in the east-north-up coordinate frame. So there is a constant error term in the eastward velocity, which is called ''sculling error''. So both eastward velocity error curves increase almost linearly with time due to the sculling error propagation.

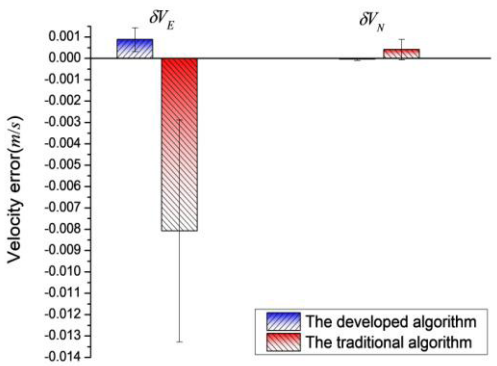

FIGURE 2. Comparison of the statistical characters of the velocity error between two algorithms.

However, both the V_E error and the V_N error of the proposed algorithm is approximately reduced by 10 times compared with those of the traditional algorithm. This is because the proposed sculling algorithm can calculate out the velocity directly without dimension conversion of inertial sensor outputs. Therefore, the sculling correction has been compensated more effectively and the velocity determination precision is improved dramatically.

To further illustrate the accuracy of the proposed algorithm, we make a quantitative comparison. The results of comparison are given in table 2:

For straight comparison, we draw a bar graph named Fig.2, based on the data of table 2:

We also compared the attitude errors of two algorithms. The results are given in Fig.3:

TABLE 2. Comparison of the statistical characters of the velocity error between two algorithms.

Errors / Algorithms	Eastward velocity error (V_E)		Northward velocity error (V_N)	
	Mean (m/s)	Variance (m^2/s^2)	Mean (m/s)	Variance (m^2/s^2)
The developed algorithm	8.78e-004	3.18e-007	-4.46e-005	2.73e-009
The traditional algorithm	-8.08e-003	2.69e-005	4.11e-004	2.31e-007

TABLE 3. Comparison of the statistical characters of the attitude error between two algorithms.

Errors / Algorithms	Roll error($\delta\gamma$)		Pitch error($\delta\theta$)		Head error($\delta\psi$)	
	Mean (°)	Variance $(°)^2$	Mean (°)	Variance $(°)^2$	Mean (°)	Variance $(°)^2$
The developed algorithm	-1.85 e-006	8.47 e-012	-1.33 e-009	5.04 e-018	1.15 e-006	1.38 e-012
The traditional algorithm	1.70 e-005	3.07 e-010	1.23 e-008	4.27 e-016	-1.06 e-005	1.17 e-010

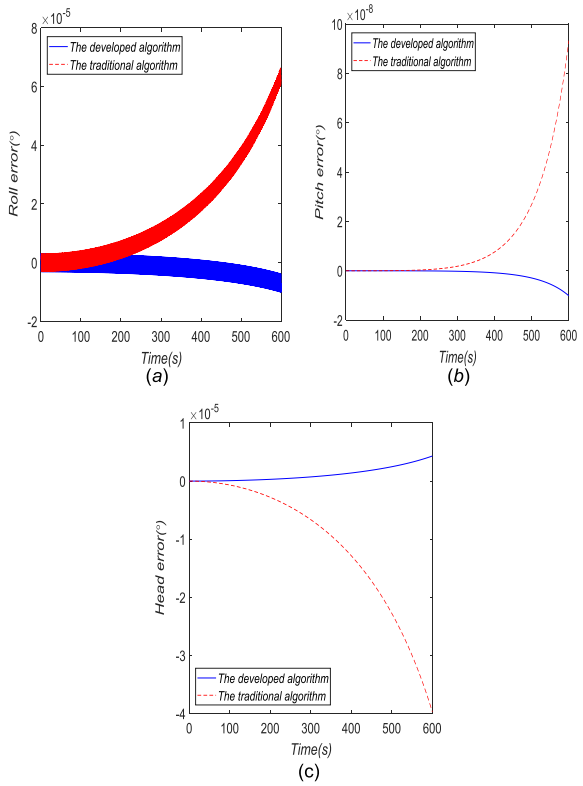

FIGURE 3. Comparison of the attitude determination results between two algorithms under sculling environment. (a) Roll error. (b) Pitch error. (c) Head error.

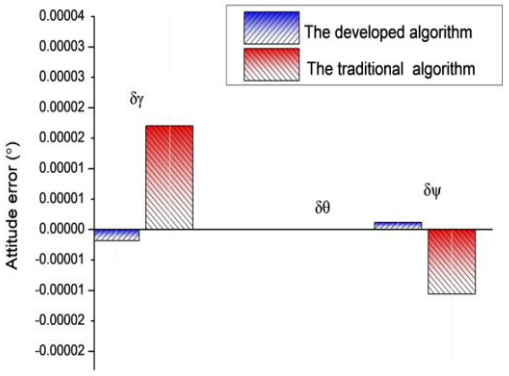

FIGURE 4. Comparison of the attitude determination results between two algorithms under sculling environment.

As is seen in Fig.3, the attitude errors of the developed algorithm are much less than those of the traditional algorithm. This is because the improved precision in velocity determination can also result in the improvement of the precision of attitude determination.

To further illustrate the accuracy of the developed algorithm, we make a quantitative comparison. The results of comparison are given in table 3 and Fig. 4:

In Fig.4 the bar of pitch error $\delta\theta$ is invisible because the pitch errors of both algorithms are so small (seen in table 3) that actually they can be neglected compared with the roll error and head error.

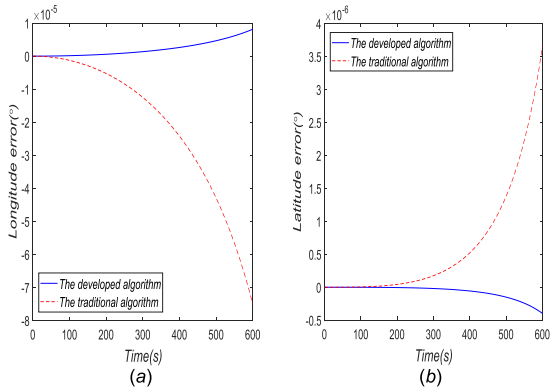

FIGURE 5. Comparison of the horizontal position determination results between two algorithms under sculling environment. (a) Longitude error (b) Latitude error.

TABLE 4. Comparison of the statistical characters of the position error between two algorithms.

Errors / Algorithms	Longitude error($\delta\lambda$)		Latitude error (δL)	
	Mean (°)	Variance $(°)^2$	Mean (°)	Variance (°)
The developed algorithm	2.18e-006	4.94e-012	-6.62e-008	9.00e-015
The traditional algorithm	-2.01e-005	4.19e-010	6.09e-007	7.62e-013

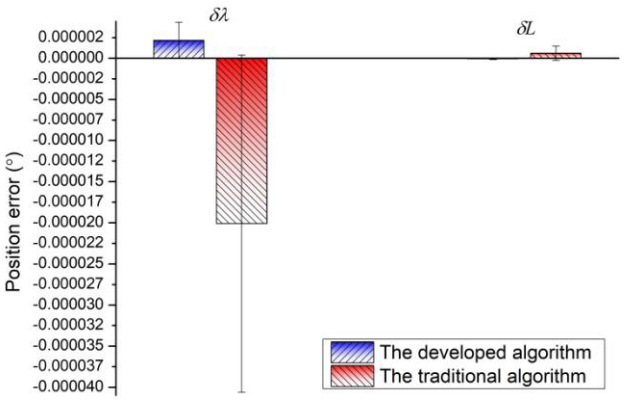

FIGURE 6. Comparison of the statistical characters of the position error between two algorithms.

We also compare the position error of two algorithms. The results are given in Fig. 5:

To further illustrate the accuracy of the developed algorithm, we make a quantitative comparison. The results of comparison are given in table 4 and Fig.6 :

From Figs.5-6 and table 4 we can see that the longitude errors of both algorithms are larger than the latitude errors of them. This is because the eastward velocity error is the key cause for the longitude error. As mentioned above, the eastward velocity errors of both algorithms are larger about one order than those northern velocity errors. However, the position errors of the proposed algorithm are reduced by about one order of magnitude compared with those of the traditional sculling algorithm. This is because the improved precision in velocity determination will also improve the precision of position determination.

VI. CONCLUSIONS

To solve the issue that in certain situations the dimensions of the IMU output do not meet the demand of the conventional sculling algorithms for input, the optimal sculling algorithms using angular rate/specific-force and angular rate/specific-force increments inputs are developed in this paper. The developed sculling algorithms can directly calculate out the velocity of the carrier without the dimension conversion of inertial sensor outputs. Accordingly, the developed algorithms provide higher precision than conventional sculling algorithms in the SINS in which the employed gyro has an angular rate output. Our novel sculling velocity algorithm thus has great useful value in such cases.

APPENDIX: THE DERIVATION OF DUALITY EQUIVALENCY BETWEEN CONING INTEGRAL AND SCULLING INTEGRAL

Let us define a vector U_1 to be the integral of the cross product of two vectors V_1 and v_1:

$$U_1 = \int (V_1 \times v_1)dt \tag{A1}$$

where $V_1 = \int v_1 dt$. Similarly, let U_2 be the integral of $V_2 \times v_2$, where v_2 is another arbitrary vector:

$$U_2 = \int (V_2 \times v_2)dt \tag{A2}$$

where $V_2 = \int v_2 dt$. Because U_1 and U_2 have identical mathematical forms, U_2 equals U_1 when v_1 in U_1 is replaced by v_2.

Now define the following:

$$v_3 \equiv v_1 + v_2 U_3 = \int (V_3 \times v_3)dt \tag{A3}$$

where:

$$\begin{aligned} V_3 &= \int v_3 dt = \int (v_1 + v_2)dt = V_1 + V_2, \\ U_3 &= \int (V_3 \times v_3)dt = U_1 + U_2 + \int (V_1 \times v_2)dt \\ &\quad + \int (V_2 \times v_1)dt \end{aligned} \tag{A4}$$

Let:

$$U_4 = \int [(V_1 \times v_2) + (V_2 \times v_1)]dt \tag{A5}$$

Comparing Eq.(A5) with Eqs.(A1)-(A3) gives:

$$U_4 = U_3 - U_1 - U_2 \tag{A6}$$

Then U_4 can be represented as:

$$U_4 = U_1(v_3 \to v_1) - U_1 - U_1(v_2 \to v_1) \tag{A7}$$

where "A→B" represents the "B replaced by A". For example, "$v_3 \rightarrow v_1$" means that v_1 is replaced by v_3.

Let us also define $\hat{U}_1$ to be a digital integration algorithm for U_1. Similarly, $\hat{U}_2$ for U_2, $\hat{U}_3$ for U_3, and $\hat{U}_4$ for U_4. It can be followed from Eqs.(A6)-(A7) that:

$$\hat{U}_4 = \hat{U}_3 - \hat{U}_1 - \hat{U}_2 = \hat{U}_1(v_3 \rightarrow v_1) - \hat{U}_1 - \hat{U}_1(v_2 \rightarrow v_1) \tag{A8}$$

Let:

$$v_1 = \omega, v_2 = f, v_3 = \omega + f, V_1 = \int v_1 dt = \Delta\theta(t),$$
$$V_2 = \int v_2 dt = \Delta V(t), V_3 = \Delta\theta(t) + \Delta V(t) \tag{A9}$$

Then we can get:

$$\Delta\hat{\Phi} = \frac{1}{2}\int [\Delta V(t) \times \omega(t)]dt = \frac{1}{2}\hat{U}_1$$
$$\Delta\hat{V}_{sculm} = \frac{1}{2}\int [\Delta\theta(t) \times f + \Delta V(t) \times \omega]dt = \frac{1}{2}\hat{U}_4 \tag{A10}$$

Substituting Eq.(A8) into $\Delta\hat{V}_{sculm}$ of Eq.(A10) can obtain the coning integral value:

$$\Delta\hat{V}_{sculm} = \frac{1}{2}\hat{U}_4 = \frac{1}{2}[\hat{U}_1(v_3 \rightarrow v_1) - \hat{U}_1 - \hat{U}_1(v_2 \rightarrow v_1)] \tag{A11}$$

Substituting Eqs.(A9)-(A10) into Eq.(A11) gives:

$$\Delta\hat{V}_{sculm} = \Delta\hat{\Phi}([\omega + f] \rightarrow \omega) - \Delta\hat{\Phi} - \Delta\hat{\Phi}(f \rightarrow \omega) \tag{A12}$$

ACKNOWLEDGMENT

The authors would like to acknowledge postgraduate student Di Sang for his work in the digital simulations. They also gratefully acknowledge the helpful comments and suggestions of English editors and reviewers.

REFERENCES

[1] P. G. Savage, "Strapdown inertial navigation integration algorithm design part 2: Velocity and position algorithms," *J. Guid., Control, Dyn.*, vol. 21, no. 2, pp. 208–221, 1998.
[2] P. G. Savage, "Strapdown sculling algorithm design for sensor dynamic amplitude and phase-shift error," *J. Guid., Control, Dyn.*, vol. 35, no. 6, pp. 1718–1729, 2012.
[3] P. G. Savage. (2016). *Digital Integration Algorithm Error For Random Process Inputs*. [Online]. Available: http://www.strapdown-associates.com
[4] M. Ignagni, "Optimal sculling and coning algorithms for analog-sensor systems," *J. Guid. Control Dyn.*, vol. 35, no. 3, pp. 851–860, 2012.
[5] M. B. Ignagni, "Duality of optimal strapdown sculling and coning compensation algorithms," *Inst. Navigat.*, vol. 45, no. 2, pp. 85–95, 1998.
[6] M. Ignagni, "Efficient class of optimized coning compensation algorithms," *J. Guid., Control, Dyn.*, vol. 19, no. 2, pp. 424–429, 1996.
[7] K. M. Roscoe, "Equivalency between strapdown inertial navigation coning and sculling integrals/algorithms," *J. Guid., Control, Dyn.*, vol. 24, no. 2, pp. 201–205, 2001.
[8] Y. A. Litmanovich, V. M. Lesyuchevsky, and V. Z. Gusinsky, "Two new classes of strapdown navigation algorithms," *J. Guid., Control, Dyn.*, vol. 23, no. 1, pp. 34–44, 2000.
[9] M. Song, W. Wu, and J. Wang, "Error analysis of classical strapdown velocity integration algorithms under maneuvers," *J. Guid., Control, Dyn.*, vol. 36, no. 1, pp. 332–337, 2013.
[10] M. Song and W. Wu, "A new digital algorithm for the velocity translation vector," *Sci. China Inf. Sci.*, vol. 56, no. 8, pp. 1–13, 2013.
[11] M. Wang, W. Wu, J. Wang, and X. Pan, "High-order attitude compensation in coning and rotation coexisting environment," *IEEE Trans. Aerosp. Electron. Syst.*, vol. 51, no. 2, pp. 1178–1190, Apr. 2015.
[12] Y. Yang and H. Zhang, "Two interval sculling compensation algorithm based on duality principle," *J. Beijing Univ. Aeronaut. Astronaut.*, vol. 35, no. 3, pp. 326–329, 2009.
[13] R.-H. Zhang, Z.-C. He, H.-W. Wang, F. You, and K.-N. Li, "Study on self-tuning tyre friction control for developing main-servo loop integrated chassis control system," *IEEE Access*, vol. 5, pp. 6649–6660, 2017.
[14] Z. Zhang, F. Zhang, and W. Zhang, "Measurement of phase difference for micromachined gyros driven by rotating aircraft," *Sensors*, vol. 13, no. 8, pp. 11051–11068, 2013.
[15] H. Li, J. Zhang, J. Shen, and X. Luo, "The improvement and optimization of sculling compensation algorithms for fiber-optical gyro sins," *J. Projectiles, Rockets, Missiles Guid.*, vol. 31, no. 6, pp. 15–22, 2011.
[16] L. Wang, L. Fu, and M. Xin, "Sculling compensation algorithm for SINS based on two-time scale perturbation model of inertial measurements," *Sensors*, vol. 18, no. 1, pp. 282–298, 2018.
[17] L. Xing, Z. Xiong, J. Y. Liu, and Y. J. Hang, "Improved coning and sculling error compensation algorithms based on dual quaternion for strapdown inertial navigation system," (in Chinese), *Acta Armamentarii*, vol. 38, no. 7, pp. 1336–1347, 2017.
[18] J. S. Peng and Y. M. Shao, "Intelligent method for identifying driving risk based on V2V multisource big data," *Complexity*, vol. 2018, no. 1, pp. 1–9, May 2018.
[19] Y. Ben, F. Sun, W. Gao, and F. Yu, "Generalized method for improved coning algorithms using angular rate," *IEEE Trans. Aerosp. Electron. Syst.*, vol. 45, no. 4, pp. 1565–1572, Oct. 2009.
[20] C. W. Kang, N. I. Cho, and C. G. Park, "Approach to direct coning/sculling error compensation based on the sinusoidal modelling of IMU signal," *IET Radar, Sonar Navigat.*, vol. 7, no. 5, pp. 527–534, Jun. 2013.
[21] H. Yang, W. Li, C. Luo, J. Zhang, and Z. Si, "Research on error compensation property of strapdown inertial navigation system using dynamic model of shearer," *IEEE Access*, vol. 4, pp. 2045–2055, 2016.
[22] P. G. Savage. (May 31, 2015). *Computational Elements for Strapdown Systems*. [Online]. Available: https://www.strapdownassociates
[23] G. Yan, J. Wang, and X. Zhou, "High-precision simulator for strapdown inertial navigation systems based on real dynamics from GNSS and IMU integration," in *Proc. 6th China Satell. Navigat. Conf. (CSNC)*, Xian, China, 2015, pp. 789–799.
[24] J. Peng, C. Wang, Y. Shao, and J. Xu, "Visual search efficiency evaluation method for potential connected vehicles on sharp curves," *IEEE Access*, vol. 6, pp. 41827–41838, 2018.
[25] T. Zhang, K. Chen, W. Fu, Y. Yu, and J. Yan, "Optimal two-iteration sculling compensation mathematical framework for SINS velocity updating," *J. Syst. Eng. Electron.*, vol. 25, no. 6, pp. 1065–1071, Dec. 2014.
[26] F. Xie, R. Sun, G. Kang, W. Qian, J. Zhao, and L. Zhang, "A jamming tolerant BeiDou combined B1/B2 vector tracking algorithm for ultra-tightly coupled GNSS/INS systems," *Aerosp. Sci. Technol.*, vol. 70, no. 1, pp. 265–276, 2017.
[27] Y.-J. Kim, "A kinematic analysis of sculling motion for prevent water safety accident," *J. Sport Leisure Stud.*, vol. 58, no. 2, pp. 881–888, 2014.
[28] Z. Li, Y. Gong, and J. Wang, "Optimal control with fuzzy compensation for a magnetorheological fluid damper employed in a gun recoil system," *J. Intell. Mater. Syst. Struct.*, p. 1045389X17754258, 2018.
[29] J. Li, C. J. Hu, L. P. Hou, and J. Liu, "Research on the SINS algorithm based on spiral vector," in *Proc. 15th Annu. Conf. Chin.-Soc.-Micro-Nano-Technol. (CSMNT)*, 2014.

LEI HUANG was born in Baoji, China, in 1975. He received the Ph.D. degree in detection technology and automatic equipment from the Nanjing University of Aeronautics and Astronautics in 2015.

Since 2007, he has been a Lecturer with Nanjing Forestry University, Nanjing, China. His research interests include the Internet of Things, strapdown inertial navigation, optical fiber gyro signal processing, and robotic systems.

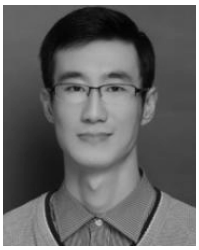

FEI XIE received the Ph.D. degree from the Nanjing University of Aeronautics and Astronautics, China, in 2014. He is currently an Assistant Professor with the School of Electrical and Automation Engineering, Nanjing Normal University, China. His current research focuses on inertial navigation, GNSS receiver signal processing, GNSS/INS-integrated navigation system, and its applications.

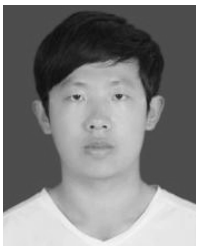

KAI FENG is currently pursuing the degree with Nanjing Forestry university, Nanjing, China. His research focuses on gesture recognition and inertial navigation technology.